Polyvinyl Alcohol Fuller's Earth Clay Nanocomposite Films

Pratibha Pandey,[1] Arup Ranjan Bhattacharyya,[2] Pranav Kumar Gutch,[1] Ram Singh Chauhan,[1] Satish Chandra Pant[1]

[1]*Defence R&D Establishment, Jhansi Road, Gwalior, India*
[2]*Department of Metallurgical Engineering and Material Science, Indian Institute of Technology Bombay, Mumbai, India*

Received 30 October 2007; accepted 22 October 2008
DOI 10.1002/app.31399
Published online 30 October 2009 in Wiley InterScience (www.interscience.wiley.com).

ABSTRACT: Nano fuller's earth was prepared by milling and subsequent sonication of clay. The polyvinyl alcohol (PVA) and PVA -Nano clay composite films were prepared by solution casting method. The films were characterized for their structural, mechanical, and thermal properties using electron microscopes (SEM, TEM), Tensile Tester, dynamic mechanical analyzer (DMA), thermo gravimetric analyzer (TGA), and Raman spectroscopy. The nanocomposite films showed improvement in mechanical properties, viscoelastic behavior as well as resistance towards thermal degradation. Uniform distribution of clay due to intimate interaction between clay and polymer appears to be the cause for improved properties. © 2009 Wiley Periodicals, Inc. J Appl Polym Sci 115: 3005–3012, 2010

Key words: polyvinyl alcohol; Fuller's earth clay; nanocomposite; films; mechanical properties

INTRODUCTION

Considerable efforts are being directed to evolve newer materials using nanoparticles for preparation of polymer inorganic hybrids, both with the aim of property enhancement and development of applications.[1,2] Polymer nanocomposites have been shown to provide unique combinations of mechanical and thermal properties often at very low filler weight fraction.

The improved properties of nanocomposits over conventional composite have been attributed to the intimate mixing of material at nanometer domain and the large surface area of filled particles. It is also reported that polymer crystallization near an inorganic surface produces nucleating or epitaxial effect. The behavior is known to promote growth of a different crystal phase and stabilizes the bulk crystal phase in certain cases.[3–8] Interactions both at the macro and nano level lead to property enhancement of the composites.

Sumita et al. reported dramatic improvement in the yield stress (30%) and Youngs modulus (170%) in nano clay filled polypropylene compared to micrometer clay filled polypropylene.[9] Various other combinations of polymer-clay nanocomposite have been reported in the literature with improved mechanical and thermal properties with 2–10 wt % add–on of nanoparticle filler.[6,7,10,11]

Notwithstanding to the susceptibility of polyvinyl alcohol (PVA) towards water and moisture, it is attracting a great deal of attention. Recently a method developed in France to disperse carbon nanotubes in PVA water solution and spinning fibers from it.[12–15] Baughman et al.[16] showed that high nanotube contening PVA fibers had a tensile strength half that of Kevlar® and toughness 17 times that of Kevlar® and three times that of spider silk. The resulting toughness of the fiber arises from chain extension in amorphous regions of PVA supported by rigid nanotubes functioning as crystalline blocks. Slippage between individual nanotubes within bundles might also contribute to toughness.

Recently Podsiadlo[17] et al. have reported layer by layer (LBL) assembly of PVA and montmorillonite clay resulting in multilayer nanocomposite films. The amount of clay was determine to be $\sim$ 70 wt % by TGA. The nanocmopsite displayed $\sim$ 4 times higher strength and nearly one order of magnitude higher modulus than pure PVA polymer.

Studies on excellent mechanical properties of PVA nano-composite films/fibers motivated our work on fuller's earth (FE) PVA nanocomposite. The aim of present study is to explore the possibility of synthesizing environment friendly biodegradable high strength cost effective nanocomposite films based on low cost commercially available FE clay and PVA. Such plastics are needed for environmental friendly applications like packaging materials (trash bags,

Correspondence to: P. Pandey (rkpratibha@yahoo.com).

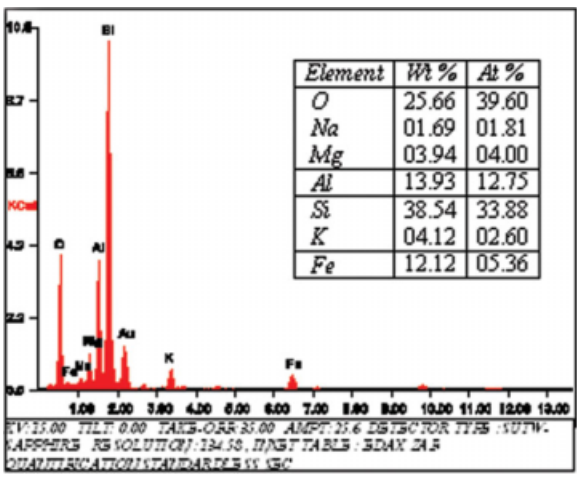

Figure 1 Composition of FE clay from SEM –EDAX analysis. [Color figure can be viewed in the online issue, which is available at www.interscience.wiley.com.]

wrappings, food containers), disposable nonwovens, agricultural mulch films and disposable hygiene products.[18]

In many of the earlier studies clays having layered sheet like structures were used for nanocomposite preparation. In the present study however nano fibrous clay having rod-like units has been used as the filler for composite preparation. Mechanical milling is an economical way for the preparation of nanoparticles.[19] In this work mechanical milling in combination with sonication has been employed to prepare clay nanoparticles.

EXPERIMENTAL

Materials and composite preparation

PVA, $M_w \sim 125{,}000$, 86–89% hydrolyzed was procured from SD fine chemicals. Commercially available FE (hydrated silicate of Na, Mg, K, Al, Fe) was used as filler material after the treatment described later. The composition of the clay as determined by SEM –EDAX standardless ZAF analysis is given in Figure 1. The FE used in this study is found to be composed of aluminosilicate with cation substitution of Sodium (1.8%), Potassium(2.6%), Magnesium (4%), and Iron (5.4%).

FE is a sedimentary clay. Its composition is known to vary depending upon the source. Mostly attapulgite (polygorskite), sepiolite and sometimes montmorrilonite type clay minerals are present in FE. Attapulgite $[(MgAl)_2Si_4O_{10}(OH).4H_2O]$ and sepiolite $\{(Mg_4Si_6O_{15}(OH)_2.6H_2O\}$ are fibrous clays with nano sized lath or needle like crystals as their units. These needles are 6–10 nm wide and many micron long. These clays have 2 : 1 chain structure and the acicular crystals are made up of silica tetrahedrons in two layers linked through oxygen at their longitudinal edges. The clay needles make mats, which layer together and give rise to the final layered structure of clay.

FE clay was wet ground in a planetary ball mill (Intel systems, India). Twenty gram of clay was mixed with 60 mL distilled water and then placed in tungsten carbide coated bowl and milled using twenty-five 10 mm diameter tungsten balls at 250 rpm for 20 h. Before mixing with PVA solution, 5% aqueous suspension of milled clay was sonicated for 15 min. PVA solution was prepared by dissolving weighed amount of PVA in distilled water at 90°C under constant stirring for 6 hrs to get homogenous solution. Clay suspension was then added to PVA solution cooled to room temperature (RT). The resulting solution was again sonicated for 15 min to ensure uniform dispersion of clay.

The solution was then cast on glass petridishes and allowed to dry at 30°C for 72 h. The films were further subjected to drying at 80°C for 72hrs under vacuum. All films were cast from solutions having final PVA concentration of 5% and with varying amount of clay i.e. 5, 10, 20, and 40%, which are termed as PFSM1, PFSM2, PFSM3, PFSM4 respectively.

Mechanical properties

Tensile properties of PVA and its composite films were evaluated with Miniaturized Tensile Tester from Rheometric Science (USA) at 50% strain rate with a specimen test length of 15 mm, width 10 mm and thickness around 75 μm. The films were conditioned at 27°C and 50% ± 5% relative humidity (RH) before testing.

Dynamic mechanical analysis (DMA)

Dynamic mechanical analysis was carried out with rectangular samples (length 5mm, width 4mm and thickness around 350 μm) using Trite 2000 DMA (Triton Technology UK) in tension mode using a dynamic frequency of 1 Hz from 0°C to 120°C at a temperature gradient of 4 K/min. The films were conditioned at 27°C and 50% ± 5% RH before testing.

Thermal gravimetric analysis (TGA)

Thermal gravimetric analysis was carried out on a TA instrument TGA-295 in nitrogen atmosphere. The temperature was ramped from RT to 800°C at 10°C/min.

Electron microscopy (SEM,TEM)

The broken film end specimens, which were subjected to tensile test, were collected. The cryofractured surfaces as well as tensile fractured surfaces were mounted on specimen stubs and coated with a

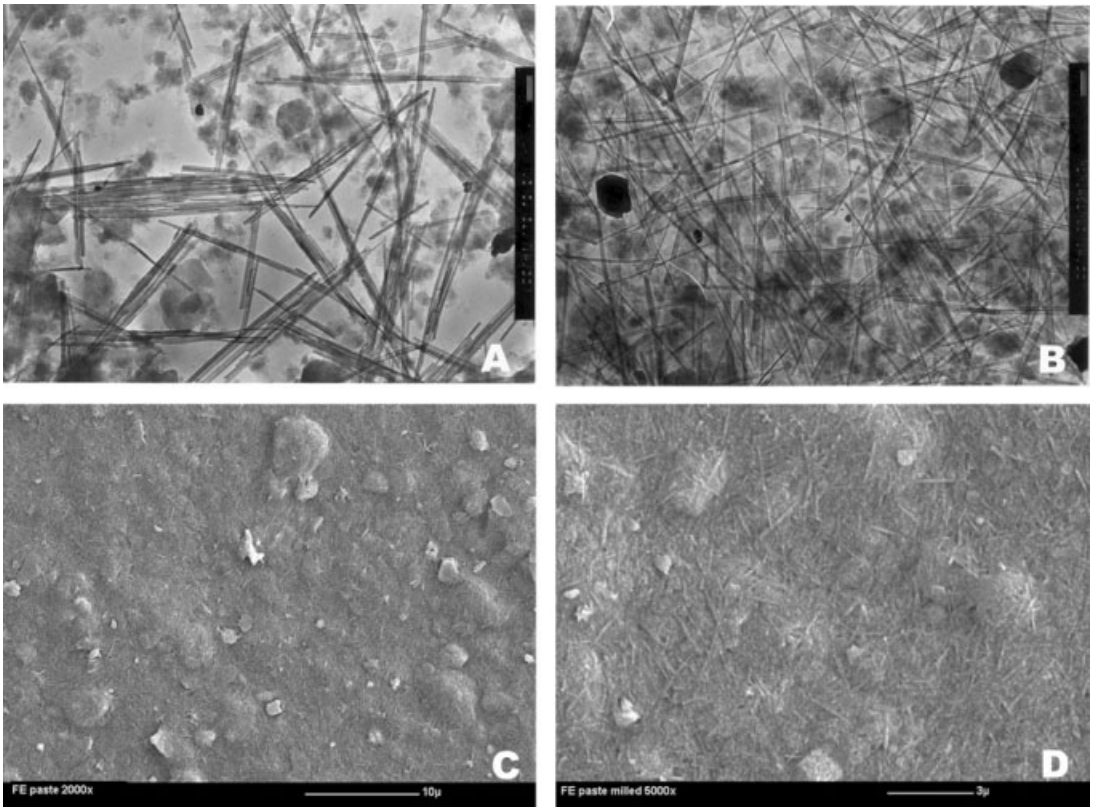

Figure 2 A,B: TEM micrograph of clay at 20,000×, (A) milled (B) sonicated for 30 min after milling. C,D: SEM micrographs of milled clay at 2000× and 5000×.

thin layer of gold before observation in the Jeol JSM 840 scanning electron microscope at 5 kV. The milled clay and sonicated clays were analyzed with SEM as well as Jeol JEM 1200 EX transmission electron microscope. For TEM clay was suspended in water and a small drop of suspension was than deposited on the carbon coated copper grid. The elemental composition of the clay was analyzed with the help of FEI Quanta 400 ESEM equipped with Energy Dispersive X-ray analyzer for elemental analysis.

Laser Raman spectroscopy

Laser Raman spectra of PVA as well PVA-Clay nano-composite films were taken Renishaw In-Via Laser Raman Microscope to establish interaction between the FE clay filler and PVA matrix. The spectra were recorded using 785 nm Laser source at 20 × magnification in standard mode and 10% laser power in the range of 3000 cm^{-1} – 4000 cm^{-1} for all the specimens.

Dispersion of prepared films in water

To determine the state of dispersion of nano clay in the composite film a water dispersion test was carried out. The test used as an indication of dispersed state of particles as individual or agglomerates. Small film samples of PVA-clay composite films with 5, 10, 20, and 40% clay loading and all having equivalent amount of clay (0.25 g) were dissolved in 20 mL of distilled water each. The clay from the films gets dispersed in the DW. The suspension so obtained is kept for 48 hrs and than observed for stability of dispersion.

RESULTS AND DISCUSSION

Figure 1 shows the elemental composition of FE clay used as the nano filler. The clay is composed of aluminosilicate with cation substitution of magnesium, iron, sodium, and potassium.

Figure 2(A–D) shows the TEM and SEM micrographs of the milled as well as milled and subsequently sonicated clay. The milled FE showed needle or fibril like units. Figure 2(A,B) show the TEM micrograph of milled clay before and after sonication at 20,000×. The particles of the clay showed stacked needle like structure with high aspect ratio of 10 to 40. The length of the clay particles varied between 2 and 5 microns and the width between 100 and 200 nm [Fig. 2(A)] with aspect ratio of 10–50. The SEM micrographs [Fig. 2(C,D)] show the uniform distribution of size and shape of clay needles.

TABLE I
Mechanical Properties of PVA and PVA-Clay Composites

% Clay loading	Yield strength (MPa)	Tensile strength at break (MPa)	Elongation at break (%)
0	79	80	220
5	91	80	100
10	100	83	100
20	105	98	40
40	70	72	6

After sonication the length and width of the acicular clay particles reduced. The width registered a value of 20–25 nm. Likewise the length also showed reduction to lower values as compaired to milled sample.

Incorporation of clay to the polymer resulted in composite films having superior mechanical properties. Table I presents the mechanical response of PVA-clay nanocomposite at different levels of clay loading. It is rather interesting to note that the filled clay improves the yield strength of the sample from an initial value of 79–100 MPa, while the tensile strength at break remains same up to 10% loading. The elongation at break however reduced to 100% from an initial value of 220% for the unfilled matrix. With further increase in the clay loading to 20% though the yield stress increased marginally to 105 MPa, the tensile strength at break registered a value of 98 MPa with a substantial reduction in elongation at break. Still higher loading of clay (40%) in PVA reduced yield strength, tensile strength at break as well as elongation at break very significantly.

During tensile loading, at low level of elongation the specimen deforms uniformly, which resulted in a steady increase in load with increasing elongation. It is well known that the cross-section of the sample decrease with increasing extension and the resulting load reaches its maximum value at the instant the uniform extension of the sample stops. Structural changes in the specimen due to further extension result in the formation of neck with a substantial fall in load. All the clay filled samples showed distinct yield point. The magnitude of yield strength appears to be influenced by the extent of clay loading (Table I). All the samples showed a uniform deformation on subsequent extension of the specimen.

Figure 3 shows the cross-sectional morphology of the specimens that have been subjected to tensile loading till fracture (3A–3D) as well as cryo-fractured cross sections (3E–3H). The PVA control films (3A) shows parallel grooves along the direction of loading. These contiguous, parallel elements were generated during tensile loading, as the original unstressed film was devoid of these patterns and revealed uniform and smooth surface (not shown). It is known that polymeric materials generate fibrillar structure when drawn. In the present case these specimen registered 200% elongation at break. And these patterns point perhaps to similar phenomenon.

The cross-sectional surface after tensile fracture for 5% clay-PVA composite (3B) revealed an entirely different pattern. The parallel, segmented pattern changed to dense nodular pattern distributed through out the width of the film. The nodular pattern however was more or less aligned in the direction of tensile loading. At higher magnification these globules appear fused-together, with small interfacial gaps at places. The fusion of globules indicates good lateral cohesion.

Figure 3(C) shows the tensile fractured cross-section of 10% clay-PVA composite. The cross-section shows the globular pattern similar to 5% loading. However the size of the nodules appeared small with larger and deeper interfacial gaps at places. Figure 3(D) (20% clay) revealed still smaller nodules clumped together to form lateral continuity. There are larger and deeper interfacial discontinuities in between gaps. The overall oriented pattern of nodules in the draw direction retained, however the localized domain showed discontinuity and separation.

Murthy et al.[20] reported presence of modular structure in a natural and nitrile rubber blend membrane formed perhaps due to colescenene of dispersed components at microscopic level during blending and mixing. The blending and mixing processes normally generate recoil of rubbery components due to differential interfacial mobility.

The fracture pattern provided insight in to the altered morphology as a result of clay incorporation and its influence on the mechanical response of the composite.

The unfilled PVA, which registered 220% elongation, had parallel and continuous segments in the direction of the stress. Incorporation of the clay resulted in the formation of nodules in the stressed sample. These nodules appeared to have formed due to the phase segregation that may set in due to elastic recoil generated at the time of specimen fracture during tensile testing. It is known that an "interphase zone" is created around the nanoparticles in a polymer matrix and these zones have properties different from bulk polymer. These interphase zones alter the polymer chain dynamics due to the intimate contact with the nanoparticles. It is expected that elastic recoil experienced by the bulk polymer matrix and the polymer chains present in the zone surrounding the clay particles will vary in magnitudes. Because of the relatively large volume fraction of interfacial polymer in even moderately filled nanocomposites the interface zones occupy considerable volume fraction in the composite and influence the chain dynamics.

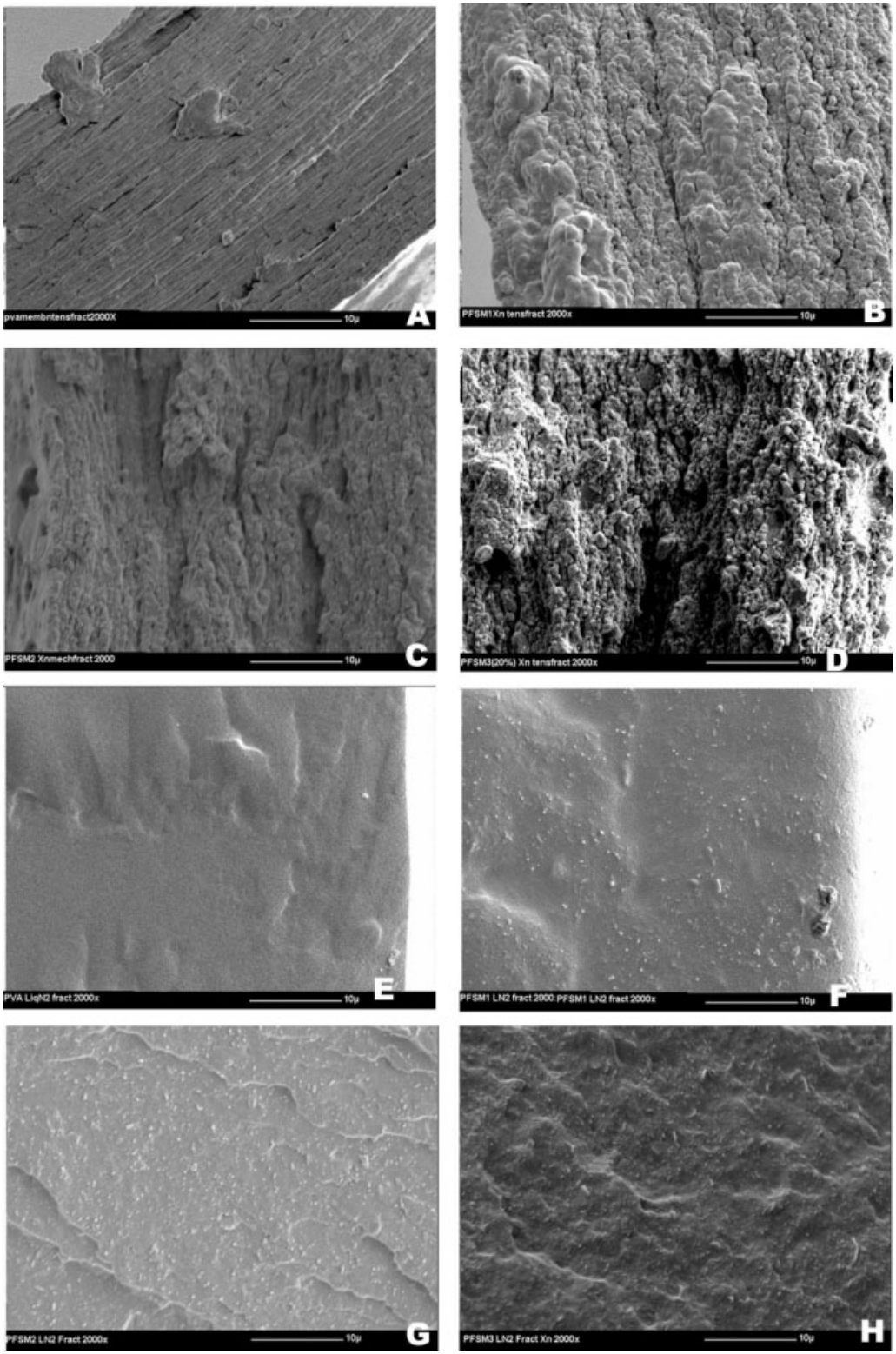

Figure 3 (A–D): Tensile fractured cross-section (Xn) surfaces of PVA and PVA clay composite films. (E–H): Liq. Nitrogen fractured cross-section surfaces of PVA and PVA clay composite films.

The reduction in the nodule size with increasing add-on is perhaps due to restricted interfacial mobility because of enhanced surface area of the clay particles. At 40% clay add-on the globular morphology changed to fibrillar one (micrograph not shown); indicating segregation of polymer and clay phases to a very great extent. The fibriller structure can be considered as PVA-coated bundles of clay particles.

The needle like clay particles have comparatively lower surface area than nanosheet clays and hence lesser agglomeration tendency as well as better dispersion in matrix. Additionally the mechanical potential (reinforcement) of fibers is higher than that of sheets.[21–23]

Figure 3(E–H) are the cryofractured section of PVA and composite films. These micrographs show the broken ends of clay needles in form of small dots in polymer matrix. The number of these clay particles increases with increasing clay loading till 10% add-on. However at 20% loading proportionate increase in number of individual dots was not noticeable. This is perhaps due to the agglomeration of clay needles at higher loadings.

This concept of agglomeration at higher clay loading is supported by the dispersion behavior of PVA-clay composite films in distilled water. It was observed that all the PVA + clay (PFSM1 to PFSM4) dispersed uniformly making a colloidal clay suspension (brownish in color), which remained stable even after 48 h. But in each case there was some residual clay present at the bottom of clay PVA suspension that represented degree of agglomeration. The amount of this residue increased with increasing clay loading. In PFSM 4 the residue was maximum and the suspension was least colored due to lowest amount of individual colloidal clay particles. These observation indicate that the clay was dispersed as uniform individual needle at lower loadings but with increasing add-on clay shows a tendency of agglomeration which is reflected in form of larger residue. In PFSM4 the agglomeration was maximized while no. of individual clay needles reduced. This phenomenon is reflected in the form of deterioration in mechanical properties at higher clay loadings i.e. beyond 20%.

Figure 4 shows Raman spectra of polymer, clay and nanocomposite films. The Raman spectra of —OH group of PVA film, FE clay and PVA-Nanoclay composite films also supports interaction

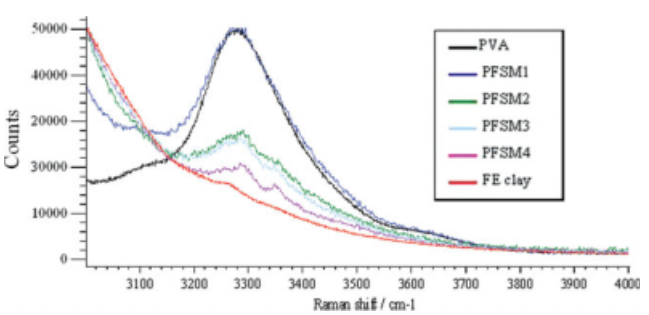

Figure 4 Raman spectra of PVA, FE clay, and PVA-nanoclay composite films. [Color figure can be viewed in the online issue, which is available at www.interscience.wiley.com.]

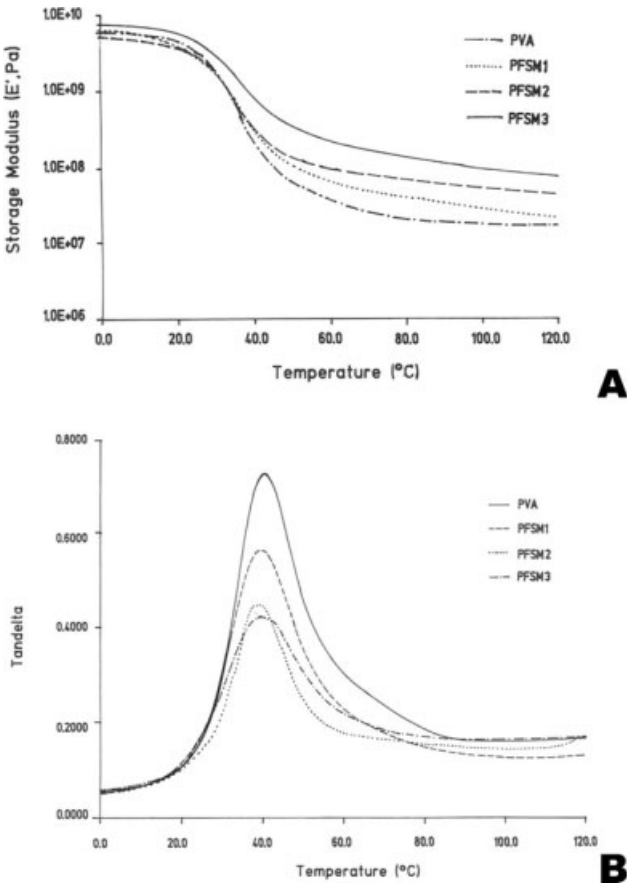

Figure 5 Viscoelastic behavior of PVA and composite films, (A) storage modulus (B) inelastic spectra.

between C—O—H group of PVA with clay which is reflected in form of suppression of C—O—H peak at 3290 cm^{-1} and appearance of a new peak at 3350 cm^{-1}. Similar results in FTIR of PVA-MTM nanocomposite were reported by Podsiadlo et al.[17]

Figure 5(A) displays the storage module spectra for the unfilled and FE filled PVA polymer. The unfilled polymer had higher storage modules in the glassy region and remained so up to 20°C than for 5 and 10% nanoclay filled composite. The 20% filled clay however showed higher storage modules than rest of the specimen. At temperature around T_g the storage modules for all the samples reduced significantly.

Table II shows the values of storage modules at different temperatures for clay filled and unfilled PVA. It is evident that the fall in the storage modules was lower for clay filled samples compared to unfilled PVA, indicating higher resistance to deformation and retention of large proportion of stiffness seen below transition as a result of clay incorporation. Presence of the nanoclay improves polymer stiffness above T_g. Similar trends have been reported in previous studies for PVA-CNT[24] and cellulose nanofiber-amorphous rubber matrix.[25]

TABLE II
Storage Modulus of PVA and PVA-Clay Composite Films

Temperature (°C)	Storage modulus (Pa)			
	PVA	5% Clay	10% Clay	20% Clay
0	6.139×10^3	4.978×10^3	5.084×10^3	6.314×10^3
20	4.196×10^3	3.534×10^3	3.515×10^3	5.413×10^3
40	2.042×10^2	2.914×10^2	3.144×10^2	8.102×10^2
60	37.02	67.51	98.83	233.0
80	19.98	40.64	72.83	14.39
100	17.25	27.67	54.82	97.95

Figure 5(B) shows the inelastic spectra of the above samples. The tangent of the ratio of complex to real modulus (tan δ) is a measure of the damping. At T_g the unfilled PVA registered the tan δ value of 0.7297. The clay filled samples showed lower mechanical energy dissipation over this temperature region. The decrease in tan δ at T_g indicates that the incorporation of FE influences the segmental dynamics of the composite. Decrease in peak height of tan δ value (damping) and broadening of the peak with progressive add-on of FE is attributed to degree of polymer-clay interaction that may occur at their interface. It is reported that strong polymer-filler interaction will decrease the mobility and free volume of polymer chains near the particle surface.[26] The interaction results in more efficient immobilization of polymer chains around the rigid clay particles. With increasing clay add-on the greater volume fraction of the chains confine to restricted mobility. Simultaneously the fraction of the flexible matrix polymer chains reduces leading to decreased tan δ peak height at T_g. A broadening of the tan δ curves in composite materials in comparison to the neat polymer can credited to an increase in the distribution of relaxation time (T). The results of storage modules prompted us to investigate the thermal response of the material. The composite films showed higher resistance towards thermal degradation. As can be seen from Table III PVA film completely degrades at 600°C while the composite films show 11–14% residue at this temperature.

TABLE III
Thermogravimatric Analysis of PVA and PVA-Clay Composite Films – Residual Mass at Different Temperatures

Temperature (°C)	% Residual mass			
	PVA	5% clay	10% clay	20% clay
200	97.3	97.7	97.7	97.0
300	81.8	90.0	92.7	91.4
400	36.4	36.8	41.8	44.5
500	8.6	15.5	12.7	16.4
600	0	13.6	10.9	14.1
700	0	10	9.1	10.9
800	0	8.2	7.3	8.2

CONCLUSIONS

The results of this study show that incorporation of FE clay in the PVA matrix improves a host of the polymer properties, which tends to increase with increased content of the FE up to a level. The fracture morphology provided insight into the mechanical response of clay filled polymer and the clay-polymer interaction.

The cross-section of the clay filled and tensile fractured sample revealed nodular morphology. The size of the nodules appears to be dependent on the contents of the clay particles as well as the load developed on the specimen during tensile fracture. The magnitude of the developed load determines the recoil force exerted on the specimen and hence the morphology.

There is a gradual increase in the yield strength of the clay filled composite with increasing content of clay up to 20%. However, further increment affected the properties adversely, perhaps due to phase segregation and clay agglomeration leading to multiple flaw generation which resulted in the low extensibility of the sample.

Viscoelastic properties also indicate polymer-clay interaction with decreased mobility of chain molecules. Raman spectra of PVA and composite films also indicate interaction between hydroxyl group of PVA with claynanosheets. The composite films also registered improved resistance towards thermal degradation.

The authors wish to acknowledge Dr. R. Vijayaraghvan Director DRDE for permission to publish this work and Mr. Vijay Kute for experimental support.

References

1. Theng, B. K. S. Formation and Properties of Clay Polymer Complexes; Elsevier: New York, 1979.
2. Giannelis, E. P.; Krishnamoorti, R.; Manias, E. Polymers in Confined Environments; Granick, S., Ed. Springer: Berlin, 1999; Chapter 3.
3. Ou, Y.; Yang, F.; Yu, Z. J Polym Sci Part B Polym Phys 1998, 36, 789.
4. Petrovic, Z. S.; Zhang, W. Mat Sci Forum 2000, 352, 171.
5. Janigova, I.; Chodak, I. Eur Polym J 1995, 31, 271.

6. Davis, R. D.; Jarrett, W. C.; Mathias, L. J Polym Mat Sci Eng 2000, 82, 272.
7. Liu, L.; Qi, Z.; Zhu, X. J Appl Phys Sci 1999, 71, 1133.
8. Probst, O.; Moore, E. M.; Resasco, D. E.; Grady, B. P. Polymer 2004, 45, 4437.
9. Sumita, M.; Tsukihi, N.; Miyasaka, K.; Ishikawa, K. J Appl Polym Sci 1984, 29, 1523.
10. Kojima, Y.; Usuki, A.; Kawasumi, M.; Okada, A.; Kurauchi, T. T.; Kamigaito, O. J. Polym Sci Part A: Polym Chem 1993, 31, 983.
11. Kojima, Y.; Usuki, A.; Kawasumi, M.; Okada, T.; Kurauchi, T. T.; Kamigaito, O. J. Polym Sci Part B: Polym Phys 1995, 33, 1039.
12. Vigolo, B.; Penicaud, A.; Coulon, C.; Sauder, C.; Pailler, R.; Journet, C.; Bernier, P.; Poulin, P. Science 2000, 290, 1331.
13. Launois, P.; Maricci, A.; Vigalo, B.; Bernier, P.; Derre, A.; Poulin, P. J. Nanosci Nanotechnol 2001, 2, 125.
14. Vigolo, B.; Poulin, P.; Lucos, M.; Launois, P.; Bernier, P. Appl Phys Lett 2002, 81, 1210.
15. Paulin, P.; Vigalo, B.; Launois, P. Carbon 2002, 40, 1741.
16. Dalton, A. B.; Collins, S.; Munoz, E.; Razal, J. M.; Ebron, V. H.; Ferraris, J. P.; Coleman, J. N.; Kim, B. J.; Baughman, R. H. Nature 2003, 423, 703.
17. Podsiadlo, P.; Kaushik, A. K.; Arruda, E. M.; Wass, A. M.; Shim, B. S.; Xu, J.; Nandivada, H.; Pumplin, B.; Lahann, J.; Ramamoorthy, A.; Kotov, N. A. Science 2007, 318, 80.
18. Gross, R. A.; Kalra, B. Science 2002, 297, 803.
19. Lai, M. O.; Lu, L.; Laing, W. Compos Struct 2004, 66, 301.
20. Murthy, L. V. R.; Banerjee, S.; Singh, B.; Chauhan, R. S. J Appl Polym Sci 1997, 65, 731.
21. Fischer, H. Material Sci Eng C 2003, 23, 763.
22. Gusev, A. A. Macromolecules 2001, 34, 3081.
23. Van Es, M. Polymer-clay nanocomposites-the importance of particle dimensions, Ph. D. thesis, TU Delft, 2001.
24. Shaffer, M. S. P.; Windle, H. Adv Mater 1999, 11, 937.
25. Favier, V.; Dendievel, D.; Canova, G.; Cavaille, P. Acta Mater 1997, 45, 1557.
26. Tsagaropoulos, G.; Eisenberg, A. Macromolecules 1995, 28, 6067.